INTER-DISCIPLINARY PROJECT

Estimation of Probability Density Functions and Graphical Models using regularized Sparse Grids.

Karthikeya Sampa Subbarao

Technical University of Munich, Department of Informatics
Boltzmannstr. 3, D-85748 Garching bei Munich, Germany
karthikeya108@gmail.com

Advisor: **Valeriy Khakhutskyy**

Examiner: **Univ.-Prof. Dr. Hans-Joachim Bungartz**

May 2015

Contents

Abstract

In this paper, we study the application of sparse grid based methods for estimation of probability density and also device a method to coarsen the grid by identifying and removing, less important ANOVA components from the model. This process also reveals the underlying structure of the dataset. We employ Markov Chain Monte Carlo sampling for estimating the expected values of sufficient statistics of the model.

1 Introduction

Suppose we have a dataset $D = \{x_1, x_2, .., x_M\}, where x_i \in \mathbf{R}^d$ drawn from an unknown distribution $p(X)$ of a random variable X. Density estimation is the construction of an estimate $\hat{p}$ of the probability density function p based on the dataset D. Density estimation has always been a very important problem in statistics and data mining [16]. Density estimation can be used in exploration and presentation of data and can be used to solve various types of problems. Classification and Sampling are two such applications.

Density estimation methods can be parametric or nonparametric. Parametric density estimation methods assume that the form of the underlying distribution is known whereas nonparametric density estimation methods only use given data samples. There are various nonparametric density estimation methods [9]. Kernel density estimation (KDE) is the most widely used nonparametric density estimation method. The (one-dimensional) estimator $\hat{p}(x) = 1/M \sum_{i=1}^{M} K((x - x_i)/h)$ is a linear combination of kernel functions K centered at the datapoints $x_i \in D$. The performance of the estimator depends on the choice of the kernel function K and the bandwidth $h > 0$ and the selection of the bandwidth is a non-trivial task.

Despite the fact that multivariate kernel density estimation is an important technique in multivariate data analysis and has a wide range of applications, its performance worsens exponentially with high dimensional data sets, this phenomenon is called *Curse of Dimensionality*, where there is exponential growth in combinatorial optimization as the dimension of the dataset increases [1]. For thorough understanding of density estimation and its applications we refer to [14].

1.1 Grid-based Density Estimation

In Kernel Density Estimation, the evaluation of $\hat{p}(x)$ depends on the number M of data points D. Thus, in order to evaluate the estimated density function $\hat{p}(x)$, all M kernel functions centered at all data points have to be evaluated. One remedy is to divide the data into a small number of bins and place a kernel function at each bin (which is also called 'gridding the data'). However, the number of bins increases exponentially with the dimension of the data points. In practice, kernel density estimation is often limited to, say, four dimensions. Note that approaches based on Fast Fourier Transforms (FFT) also rely on grids and thus are hardly considered in more than four dimensions [3].

Density estimation methods like KDE are sensitive with respect to the parameters and have long runtime for large datasets. Grid based methods overcome these limitations to a certain extent. However, similar to KDE, full grid approach also suffers from *Curse of Dimensionality.* The number of grid points in the full grid, grows exponentially with the dimension of the data points. For more details on the grid-based methods, we refer to [13].

1.2 Sparse-Grid-based Density Estimation

As mentioned earlier, estimation of density using Grid based methods also suffer from the curse of dimensionality for higher dimensional problems. Hence we switch to a hierarchical grid instead of an equidistant grid. It is shown that we can construct a grid which retains the high accuracy of the full mesh grid with much less grid points. L2 regularised density estimation model has been developed using the Sparse Grid techniques which has proven to be effective in dealing with the curse of dimensionality [13].

Sparse grid method is a special discretization technique. It is based on a hierarchical basis, a representation of a discrete function space which is equivalent to the conventional nodal basis, and a sparse tensor product construction. For the representation of a function f defined over a d-dimensional domain the sparse grid approach employs $\mathcal{O}(h_n^{-1} \cdot log(h_n^{-1})^{d-1})$ grid points in the discretization process, where n is the discretization level and $h_n = 2^{-n}$ denotes the mesh size [2]. In depth details of the topic can be found in [6].

For clear understanding of the concept of basis functions, we refer to the comprehensive description provided in [13].

1.2.1 Hierarchical Basis

Let $\mathcal{V}_l$ be the sparse grid space of level l corresponding to the domain $\Omega = [0,1]^d \in \mathbf{R}^d$, which consists of the so called hierarchical basis. In the standard case, piecewise linear hat functions are used as basis functions. One-dimensional standard hat function $\varphi : [-1,1] \to \mathbf{R}$ is defined as

$$\varphi(x) = max(1 - |x|, 0). \tag{1}$$

The one-dimensional hierarchical hat function $\varphi_{l,i}$ centered at the grid point $x_{l,i} = i.2^{-l}$ is the result dilation and translation of φ,

$$\varphi_{l,i}(x) = \varphi(2^l x - i). \tag{2}$$

We extend the hat function to d-dimensional case by using a tensor product approach

$$\varphi_{\mathbf{l},\mathbf{i}}(x) = \prod_{j=1}^{d} \varphi_{l_j,i_j}(x_j), \tag{3}$$

where $l = (l_1, ..., l_d)$ and $i = (i_1, ..., i_d)$ denote the level and index respectively. The corresponding grid point $x_{l,i} = [x_{l_1,i_1}, ..., x_{l_d,i_d}]^T$ is the center of the support of $\varphi_{\mathbf{l},\mathbf{i}}$.

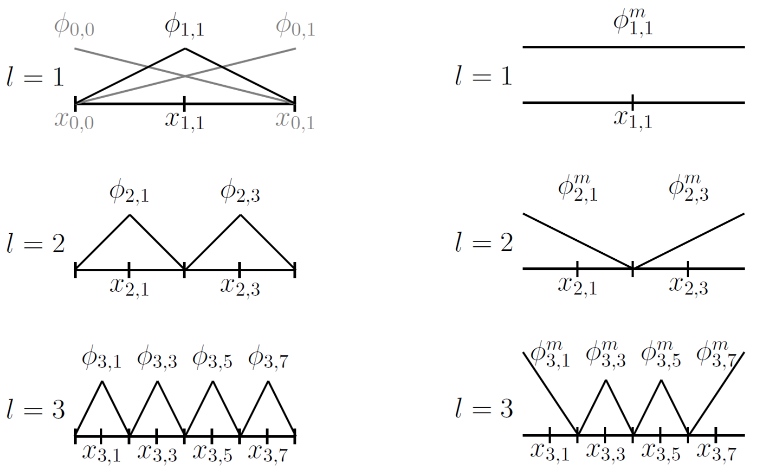

(a) hierarchical basis (b) modified/nonuniform basis

Figure 1: Hierarchical Basis Functions for level $l = 1$ to $l = 3$ are shown in (a). Modified or nonuniform basis functions are shown in (b). Source: [13].

1.2.2 Modified Linear Basis

We employ Sparse Grid with a modified linear basis for our density estimation method, since it has a correspondence to the Analysis of Variance (ANOVA) like decomposition. Above figure shows both hierarchical and modified or nonuniform basis functions. These basis functions extrapolate towards the boundary and so do not require boundary points to approximate functions with non-zero values at the boundary. The hierarchical basis function $\varphi_{l,i}$ is modified in the following way

$$\varphi^m_{l,i}(x) = \begin{cases} 1 & \text{if } l = 1, i = 1, \\ \left\{ \begin{array}{cc} 2 - 2^l \cdot x & \text{if } \ x \in [0, 2^{-(l-1)}] \\ 0 & \text{else} \end{array} \right\} & \text{if } l > 1, i = 1, \\ \left\{ \begin{array}{cc} 2^l \cdot x + 1 - i & \text{if } \ x \in [1 - 2^{-(l-1)}, 1] \\ 0 & \text{else} \end{array} \right\} & \text{if } l > 1, i = 2^l - 1, \\ \varphi(x \cdot 2^l - i) & \text{else.} \end{cases} \tag{4}$$

1.3 Analysis of Variance

We consider a decomposition of the d-dimensional function h as

$$\begin{aligned} h(x_1, ..., x_d) = h_0 + \sum_{j_1}^{d} h_{j_1}(x_{j_1}) + \sum_{j_1 < j_2}^{d} h_{j_1,j_2}(x_{j_1}, x_{j_2}) \\ + \sum_{j_1<j_2<j_3}^{d} h_{j_1,j_2,j_3}(x_{j_1}, x_{j_2}, x_{j_3}) + \cdots + h_{j_1,...,j_d}(x_{j_1}, ..., x_{j_d})). \end{aligned} \tag{5}$$

Where, h_0 is a constant function, h_{j_1} are one-dimensional functions, h_{j_1,j_2} are two-dimensional functions, and so on. This type of decomposition is known in statistics under the name analysis of variance (ANOVA) which is used to identify important variables and important interactions between variables in high-dimensional models. Note that (5) is a finite expansion of h into 2^d different terms. Such a decomposition can be gained by a tensor product construction of a splitting of the one-dimensional function space into its constant subspace and its remainder. For the detailed understanding of the topic we refer to [4].

Here we are interested in the decomposition of a sparse grid function $u \in \mathcal{V}_l$ (sparse grid space) with respect to a subspace $\tilde{\mathcal{H}}_{\mathcal{K}}$, the hierarchical subspaces of the sparse grid structure. This means, the constant function h_0 in (5) is replaced by a function $\tilde{u} \in \tilde{\mathcal{H}}_{\mathcal{K}}$ as well as all further functions $u_{j_1}, u_{j_1,j_2}, ...$ are constructed with respect to $\tilde{\mathcal{H}}_{\mathcal{K}}$. The figure $2(a)$ shows the two-dimensional ANOVA-like decomposition with respect to $\tilde{\mathcal{H}}_{(2,2)}$.

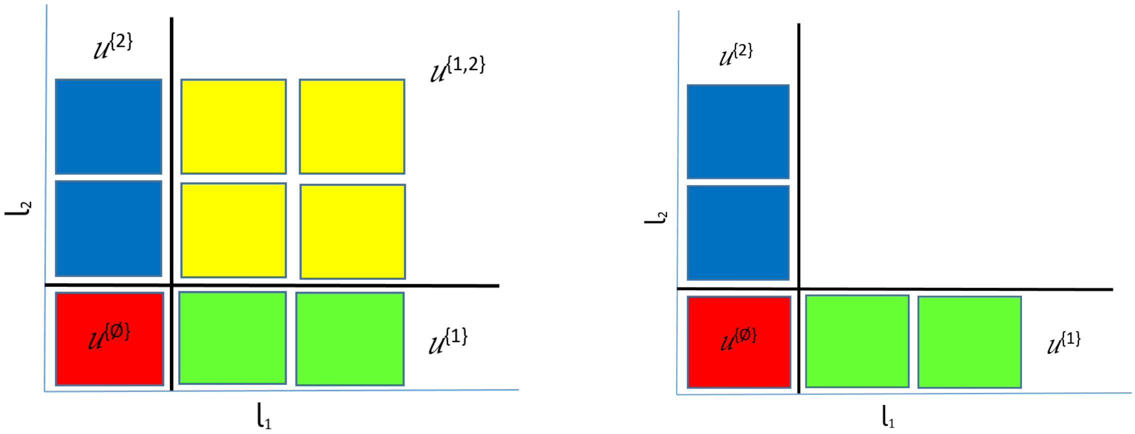

(a) (b)

Figure 2: The two-dimensional ANOVA-like decomposition with respect to $\tilde{\mathcal{H}}_{(2,2)}$: The bold cross indicates which hierarchical increments belong to which component. Figure (b) shows the decomposition after deletion of the components corresponding to a factor.

1.4 Coarsening the Grid

Now we will look into a method which can further improve the efficieny of density estimation. As stated earlier, the sparse grirds use much less grid points than the full grid. As an extension of the hypothesis, we might be able to achieve the same level of accuracy by further coarsening the grid, i.e., to delete the grid points which are less important. This can be achieved by formulating a relationship between the grid points and ANOVA components of the model. The existence of a relation between sparse grids and dimension decomposition has been studied and sparse grid approach to dimension decomposition which works similar to ANOVA decompositions has been shown in [7]. In this project we employ sparse grid with modified basis which corresponds to ANOVA like decomposition and further associate the components with the factors of a factor graph. Thus we formulate an approach to compute, analyze and visualize ANOVA components which will help us to identify unwanted or less important components and remove them in order to reduce the complexity of the problem and hence improving the computational efficiency. The figure 2(b) shows the structure after removing grid points corresponding to one of the components from the grid.

2 Density Estimation using Sparse Grid

Suppose we have an initial guess p_ϵ of the density function underlying the data, $D = \{x_1, ..., x_M\}$ and let f resemble a member of exponential family, we look for $\tilde{p}$ in the function space $\mathcal{V}$ such that

$$\tilde{p} = argmin_{f \in \mathcal{V}} \int_\Omega (f(x) - p_\epsilon(x))^2 dx + \lambda || \wedge f ||^2_{L^2}. \tag{6}$$

The left term of (6) makes sure that $\tilde{p}$ stays close to p_ϵ, the right term $||\wedge f||^2_{L^2}$ is a regularization term which imposes smoothness constraint. For instance, $\wedge$ can be chosen to be ∇. The regularization parameter $\lambda > 0$ controls the trade-off between fidelity and smoothness.

Let Ψ_l be the set of hierarchical basis functions of the sparse grid space $\mathcal{V}_l$ of level l. If we set $p_\epsilon = \frac{1}{M}\sum_{i=1}^{M} \varphi(x_i)$, we obtain after some transformations (refer [12]), the variational equation of the form

$$\int_{\Omega} \varphi(x)\hat{f}(x)dx + \lambda \int_{\Omega} \wedge \hat{f}(x) \cdot \wedge \varphi(x)dx = \frac{1}{M}\sum_{i=1}^{M} \varphi(x_i), \tag{7}$$

which holds for all $\varphi \in \Psi_l$ and $\hat{f}(x) = \frac{exp(f(x))}{\int exp(f(z))dz}$.

We discretize the function $f(x)$ using sparse grid discretization technique. The function $f(x)$ as a linear combination of basis functions is written as follows:

$$f(x) = \sum_{j=1}^{N} \alpha_j \varphi_j(x), \tag{8}$$

where N is the number of grid points. α represents the coefficients and $\varphi(x)$ represents the basis functions which is defined in section 1.2.

We use Maximum a Posteriori approach to estimate the density and we adapt the modified version of the algorithm described in [5]. One ($\mathrm{k^{th}}$) iteration of the algorithm in the mathematical form is given as

$$\sum_{j=1}^{N} \alpha_j^{i+1} a(\varphi_k, \varphi_j) = \frac{1}{M}\sum_{i=1}^{M} \varphi_k(x_i) - \int \varphi_k(x) \frac{exp(\sum_{j=1}^{N} \alpha_j^i \varphi_j(x))}{\int exp(\sum_{j=1}^{N} \alpha_j^i \varphi_j(z))dz} dx. \tag{9}$$

We can write (9) in the Matrix form as follows,

$$A_{k,j}\alpha^{i+1} = E_{empir} - \Phi(\alpha^i). \tag{10}$$

Where A represents the Regularization operator

$$A_{k,j} = a(\varphi_k, \varphi_j) = \lambda \int \bigtriangledown \varphi_k(x) \bigtriangledown \varphi_j(x)dx. \tag{11}$$

And E_{empir} can be computed using the definition of the basis functions

$$E_{empir} = \frac{1}{M}\sum_{i=1}^{M} \varphi_k(x_i). \tag{12}$$

The challenge lies in solving the following nonlinear part, which represents the expected value of the function $\varphi_k(x)$,

$$\Phi(\alpha^i) = \int \varphi_k(x) \frac{exp(\sum_{j=1}^{N} \alpha_j^i \varphi_j(x))}{\int exp(\sum_{j=1}^{N} \alpha_j^i \varphi_j(z))dz} dx. \tag{13}$$

We employ Markov Chain Monte Carlo (MCMC) sampling for computing this nonlinear term. Different approaches to solve this term, like Monte Carlo Integration has been evaluated in [15].

2.1 Computating the Expected Value using MCMC

The nonlinear term (13) can be written as follows:

$$\Phi(\alpha^i) = \int \varphi_k(x) l(x)dx. \tag{14}$$

For the sake of simplicity let us rewrite the equation as

$$\Phi(\alpha^i) = \int g(x) l(x)dx, \tag{15}$$

where $l(x) = \frac{exp(\sum_{j=1}^{N} \alpha_j^i \varphi_j(x))}{\int exp(\sum_{j=1}^{N} \alpha_j^i \varphi_j(z))dz}$ which gives the probability with which we need to sample the input values x for the function $g(x)$. Hence, (15) actually represents the expected value of $g(x)$ and can be written as

$$E[g(x)] = \int g(x)l(x)dx. \tag{16}$$

Following are the methods we employed to compute this expected value:

- We can compute the denominator of $l(x)$, i.e., $\int exp(\sum_{j=1}^{N} \alpha_j^i \varphi_j(z))dz$ using Monte Carlo Integration and use the value to compute $E[g(x)]$, which is also done with Monte Carlo Integration. This method has high runtime and hence becomes infeasible for high dimensional datasets [15].

- We can sample values from $l(x)$ using Markov Chain Monte Carlo (MCMC) by creating a model based on the Sparse Grid structure and assuming particular distribution (preferable Uniform) for the random variables. Once we sample the values from $l(x)$ using MCMC, we can evaluate the function $g(x)$ on these values and compute the mean which will be the expected value of the function $g(x)$. For computing the expected value of the function iteratively based on the updated model, we can use the sample values obtained in the previous sampling run. We can either store the sampled values and use them to initiate the sampling process in the current iteration, or we can sample few new points and compute the expected value by reusing the output of the function values from the previous iteration. Either way it should result in faster convergence of the sampling run.

2.2 Estimating the coefficients of the basis functions using MAP approach

Having discussed all the fundamental concepts, let us have a look at the basic algorithm for estimating the density underlying the given dataset. Given a d-dimensional dataset of length n and a modlinear grid, we are required to estimate the coefficients corresponding to each grid point.

At first we initialize the parameters ω, the learning rate, ϵ, a measure to compare the residual and decide when to stop the algorithm and $imax$ which represents the maximum number of iterations allowed, which in our case we set to the number of grid points.

Upon obtaining these coefficients, i.e., the α-vector, we estimate the density of the data points using,

$$d(x) = \exp\,(\sum_{i=1}^{n} \alpha_i \varphi_i(x)). \tag{17}$$

Algorithm 1: Estimating the coefficients of the basis functions using MAP approach

Data: ModLineaerGrid, Coeffecients, Set of DataPoints $X = x_1, .., x_M$
Result: Coefficients corresponding to each basis function of the grid
Choose Parameters $\omega > 0$, $\epsilon > 0 \, and \, i_{max} = Grid\ Size$;
Calculate q;
Calculate A;
Calculate $\Phi(\alpha^0)$ as describe in section 2.1;
while $residual > \epsilon$ *and* $i <= i_{max}$ **do**
  $b = q - \Phi(\alpha^i)$;
  Solve $A = \tilde{\alpha} b$;
  $\alpha^{i+1} = \alpha^i + \omega\tilde{\alpha}$;
  Calculate $\Phi(\alpha^{i+1})$ as describe in section 2.1;
  residual $= \|A\alpha^{i+1} - q + \Phi(\alpha^{i+1})\|$;
  $i = i + 1$;
end

3 Performance Improvement Strategies

3.1 Dynamic Learning Rate using Armijo Line Search

Even though having an assumed and fixed learning rate for the estimation of coefficients gave us good results, it would not suit for all kinds of problems and would take more time to converge. In order make the algorithm more efficient and reliable, we employ Armijo type line search to determine the learning rate at every iteration.

The problem that we are trying to solve is a minimization problem where we are trying to minimize the objective function which is the negative log likelihood of the given dataset. We employ Newton-Raphson procedure for minimizing the objective function. This involves determining the descent direction and the step size of the descent. Once we obtain the descent direction for our objective function, we need to pick the right step size. Taking a step too large might result in the function value being greater than the current value or if the step size is too small it might take forever to converge. Armijo's condition basically suggests that the 'right' step size is such that we have a sufficient decrease in the function value at the new point. This is mathematically represented as follows:

$$t(x_k + \omega p_k) \leq t(x_k) + c_1 \omega \nabla t_k^T p_k \tag{18}$$

where t is the function we are trying to minimize, ω is the learning rate and p_k is the descent direction at x_k and $c_1 \in (0, 1)$.

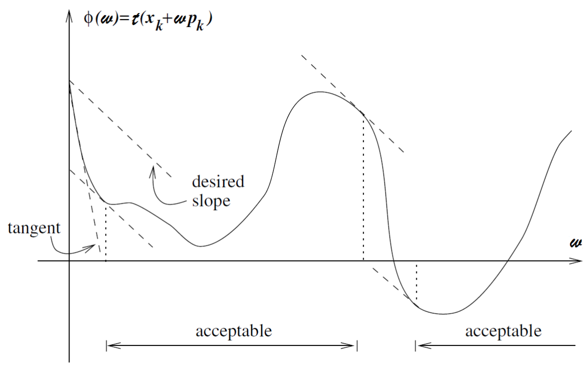

Figure 3: Armijo Condition for choosing the right step size in the descent direction. Source: [11].

The reduction in t should be proportional to both the step length ω and the directional derivative $\nabla t_k^T p_k$. The inequality (18) is sometimes called Armijo condition. For detailed understanding of the concept we refer to [11].

3.2 Grid Coarsening Strategies

As mentioned earlier in section 1.2.4, we can improve the performance of our algorithm by coarsening the grid. Now we discuss the strategy to associate the grid structure with ANOVA-like components and a method to identify the components which are less important to our model. We use *factor graph* to model the dependencies among the variables (dimensions). Initially we model the dependency of all the variables being dependent on one another by creating a fully connected factor graph. Then gradually based on the estimated coefficient values, unwanted factors are removed from the factor graph and the grid is coarsened accordingly. This will reduce the computational complexity of estimating the coefficients. Now we describe a strategy for identifying the unwanted or less important factors.

Mean Coefficient Thresholding

First step is to estimate the coefficients of all the grid points. Then we fetch and store the grid point index and corresponding factors that it is involved with. For each such factors, we list all the corresponding coefficients. If the mean of the coefficients is less than some *chosen threshold* value, then the factor is marked to be deleted. Once we have evaluated all the factors, we delete each factor in the delete list if there are no higher order factors that have this factor as a subset.

Mean Surplus Volume Thresholding

Surplus volume of a grid point represents the basis function values weighted by corresponding basis function surplus (coefficient). Surplus volume is a better measure for gauging the importance of factors in the model. Mean surplus volume thresholding strategy is same as mean coeffcient thresholding, only difference is that we use surplus volumes in place of coeffcient values.

Choosing the Coefficient Threshold

Choosing the threshold as a decision measure for deleting the dependencies from the model is non-trivial. However, experiments with few artificial datasets with known co-variance and structure helped in determining a strategy to calculate the threshold. Mean of the absolute values of all the coefficients, estimated in the very first execution of our algorithm turned to be a good choice. Similar choices with slight variations like dynamically updating the threshold at every iteration with the mean of the absolute values of the estimated coefficients corresponding to factors with atleast one iteraction, also performed well for some datasets. Algorithm 3 in section 3.3 provides implementation details.

Updating the Grid

As and when we throw away components from the factor graph / ANOVA components and drive the corresponding coefficient values to zero, we also need to update the grid accordingly by deleting the corresponding grid points. This reduction in the grid contributes to the improvement in the performance of the algorithm. Entire logic which controls the deletion of the components in the model is laid out in the form of a factor graph and driven using the coefficient values which corresponds to the components in factor graph. Hence it is possible to make sure that crucial grid points are not deleted when there are higher level grid points present in the grid;

which otherwise might lead to inconsistency in the grid. Algorithm 4 in section 3.3 provides implementation details.

3.3 Algorithms

In this section we provide the algorithms for the concepts described earlier. Algorithm 2 is the improved form of Algorithm 1 descibed earlier.

Algorithm 2: Estimating the coefficients of the basis functions - 'Newton-Raphson' procedure for penalized maximum likelihood

Data: $grid$, α, $factor\_graph$, $data$ `// Modified Linear Basis Grid`
Result: α corresponding to each basis function
Initialize Parameters: $\epsilon > 0 \, and \, i_{max}$ = size of $grid$
Calculate A
Compute E_{empir}
Calculate model expected values: $\Phi(\alpha^0)$ (section 2.1)
Compute $b = E\_empir - \Phi(\alpha^0) - A \cdot \alpha$
while $||\nabla\mathcal{L}|| > \epsilon$ *and* $i <= i_{max}$ **do**
  Solve $A = \tilde{\alpha} b$
  choose ω (section 3.1) such that $t(x_k + \omega p_k) \leq t(x_k) + c_1 \omega \nabla t_k^T p_k$
  $\alpha^{i+1} = \alpha^i + \omega * p_k$
  Calculate model expected values: $\Phi(\alpha^{i+1})$ (section 2.1)
  Compute $\nabla\mathcal{L} = E_{empir} - \Phi(\alpha^{i+1}) - A \cdot \alpha$
  $grid$, α = `grid_coarsening`($grid$, α, $factor\_graph$)
  if $grid$ updated **then**
    Update Coefficient vector, retaining only non zero values
    Calculate A
    Compute E_{empir}
    Calculate model expected values: $\Phi(\alpha^i)$ (section 2.1)
    Compute $\nabla\mathcal{L} = E\_empir - \Phi(\alpha^i) - A \cdot \alpha$
  end
  $i = i + 1$
end

Algorithm 3: Coefficient Thresholding

```
Procedure coefficient_thresholding(grid, α, factor_graph)
    Set α_t = mean of |α|
    for gp in grid do
        for d in dimension do
            if level(d) of the gp != 1 then
                factor = factor + (d)
            end
        end
        factor_alpha_collection[factor] = α[gp]
        for factor, alphas_of_factor in factor_alpha_collection do
            if mean of |alphas_of_factor| < α_t then
                add factor to delete_list
            end
        end
    end
    for factor in delete_list do
        if factor not a subset of higher order factors then
            delete the factor from the factor_graph
        end
    end
    return factor_graph
```

Algorithm 5: Grid Coarsening

```
Procedure grid_coarsening(grid, α, factor_graph)
    factor_graph = coefficient_thresholding(grid, α, factor_graph)
    for grid_point in grid do
        for d in dimension do
            if level(d) of the grid_point != 1 then
                factor = factor + (d)
            end
        end
        if factor not in factor_graph then
            α[grid_point] = 0
            delete grid[grid_point]
        end
    end
    return grid, α                              // returns coarsenend grid
```

4 Experiments and Results

We evaluate the sparse-grid based density estimation (SGDE) algorithms introduced in section 3.3 in different ways using artificial datasets and other publicly available datasets. Our artificial data sets are sampled in each direction independently from normal distribution with mean 0.5 and standard deviation 0.1. For all our experiments, we set the regularization parameter $\lambda = 10^{-1}$ (unless otherwise mentioned) since it provided the best results in our experiments. This is in contrast to the findings observed in [13], in which, setting the regularization parameter to much lesser value $\lambda = 10^{-5}$ gave best results.

Validation of density estimation results

Figure 4 shows the comparision of the density distribution of the data obtained from posterior sampling of our model and the true distribution. As one can see, our method was able to estimate the underlying distribution pretty accurately. In order to quatify the measure of accuracy we use Kolmogorov-Smirnov (KS) two-sample test [8], a nonparametric method for comparing two samples and determine whether they are from same probability distribution or different. In this case, the test returned a p-value greater than 70%, which means that we cannot reject the hypothesis that the two samples are from the same distribution.

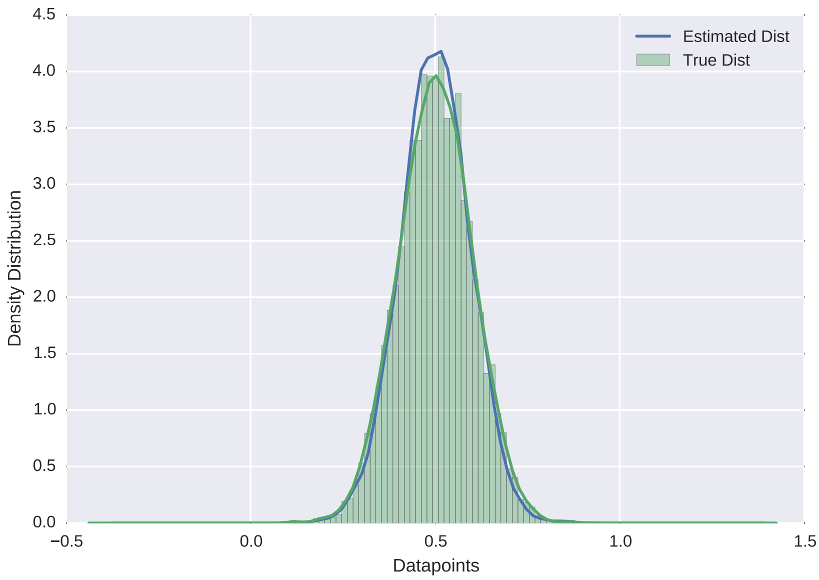

Figure 4: True and Estimated distribution of 1D Normal dataset.

In case of artificial datasets, we know the exact density function p and hence we can compute the average $\mathcal{L}_2$ error

$$\frac{1}{M_D}\sqrt{\sum_{x\in D}(p(x)-\hat{p}(x))^2}, \tag{19}$$

where M is the number of datapoints in the dataset D.

Figure 5(a) shows the comparision of $\mathcal{L}_2$ error for two multivariate normal datasets of differnt magnitude. The blue and green bar in the graph indicates the error measure for datasets with $M = 1000$ and $M = 100,000$ datapoints respectively. Note that the error corresponding to the dataset with more number of datapoints is less. This infers that our method estimates a better model when fed with more data.

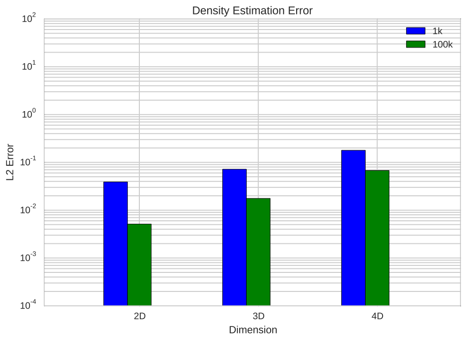

(a)

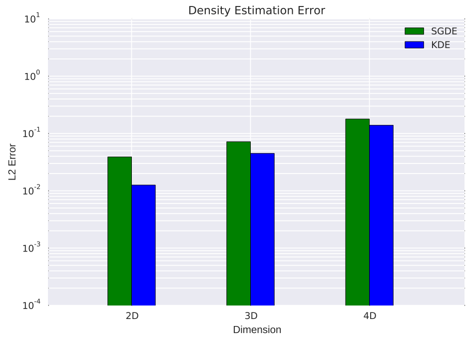

(b)

Figure 5: Comparison of our density estimation method based on sparse grids (SGDE) for datasets of different magnitude is shown in (a) and the comparision of SGDE with kernel density estimation (KDE) is show in (b). Dimensions of the datasets are marked on the x axes and y axes shows the $\mathcal{L}_2$ error.

Since statistical tests like KS test are applicable only in one-dimensional cases, we need another method to evaluate the results obtained using SGDE algorithm. Hence we compare the results with kernel density estimation (KDE) for more than one-dimensional datasets. Note that we compare our results with KDE implemented in Python Scipy [10] package which uses Silverman's rule to choose the bandwidth parameter. Figure 5(b) shows the comparision of the density estimation method based on sparse grids and kernel density estimation in terms of $\mathcal{L}_2$ error. The figure shows that there is not much difference in the performance of both of these approaches. One more observation from these graphs is that the error increases significantly with the increase in the dimension of the dataset.

Validation of estimated coeffecients

Since our algorithm is estimating the values of the coefficients corresponding to the basis functions of the sparse grid, the best way to validate our algorithm is to compare the estimated coefficient values with the true coefficient values. In case of dimensionaly independent artificial dataset, it is possible for us to compute the true coefficient values. Figure 6 shows the comparision of the coefficient values of the datasets of dimensions one, two, three and four, each having $M = 5000$ datapoints.

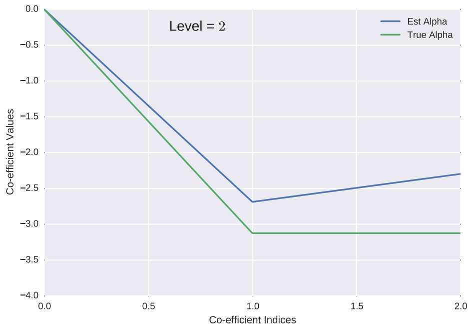

(a) one dimension

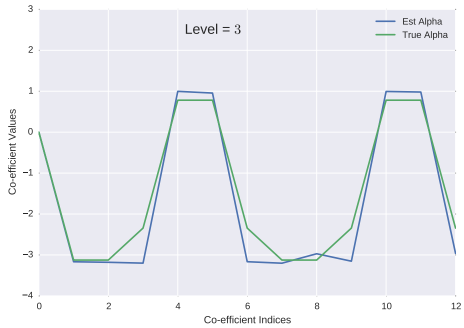

(b) two dimensions

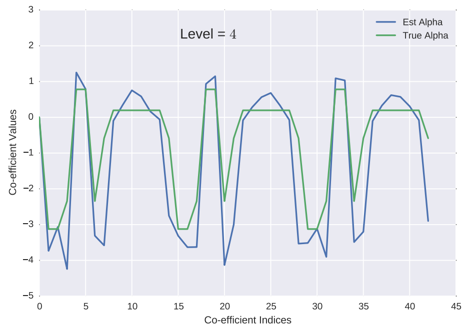

(c) three dimensions

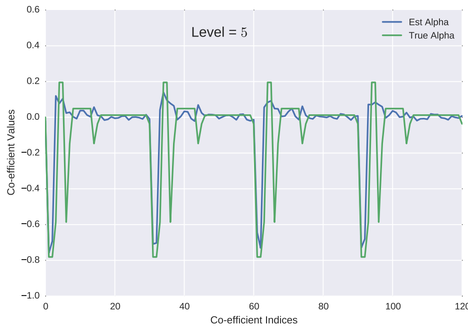

(d) four dimensions

Figure 6: True and Estimated values of the coefficients.

The estimated coeffcient values are pretty close to the true values. However, with the increase in the dimension of the dataset, the estimated values differ significantly at the points of sharp variations, which can be clearly observed in figure 6(d).

Convergence

Now we evalaute our method on two publicly available datasets. Since we do not known the exact density functions for these datasets, we analyze the behavior of the algorithm by observing the negative log likelihood and likehood gradient norm at each iteration.

Ripley dataset is a two-dimensional dataset which consists of 250 datapoints.

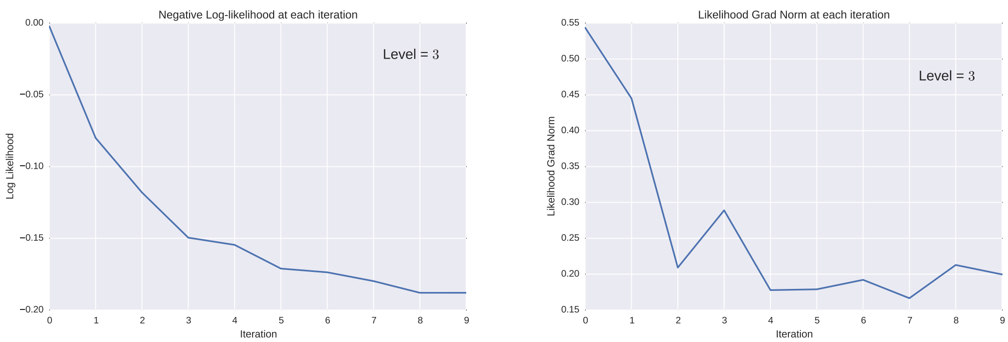

Figure 7: Negative Log-likelihood and Likelihood Gradient Norm per iteration for Ripley dataset.

The BUPA Liver Disorders data set from Irvine Machine Learning Database Repository is a six-dimensional dataset which consists of 345 datapoints.

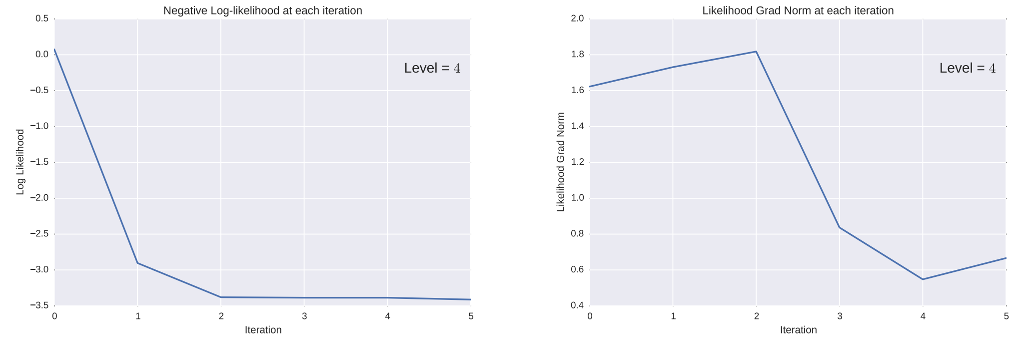

Figure 8: Negative Log-likelihood and Likelihood Gradient Norm per iteration for BUPA Liver dataset.

For both these datasets, we can see that the negative log likelihood decrease sharply in first few iterations and at further iterations it does not change much. This is an indication that the algorithm has converged. The likelihood gradient norm on the other hand can interpreted as the step size, which also decreases with the number of iterations however not as smooth as the log likelihood.

Structure of the dataset

In section 3.2 we explained strategies for coarsening the grid. Now we will see how exactly the algorithm measures the importance of the factors using surplus volume thresholding. In order to illustrate this, we generate four-dimensional normally distributed dataset with a known structure. We initiate the algorithm (2) with a 3-factor interaction factor graph model and observe how the algorithm measures the importance of individual factors gradually deletes the less important ones.

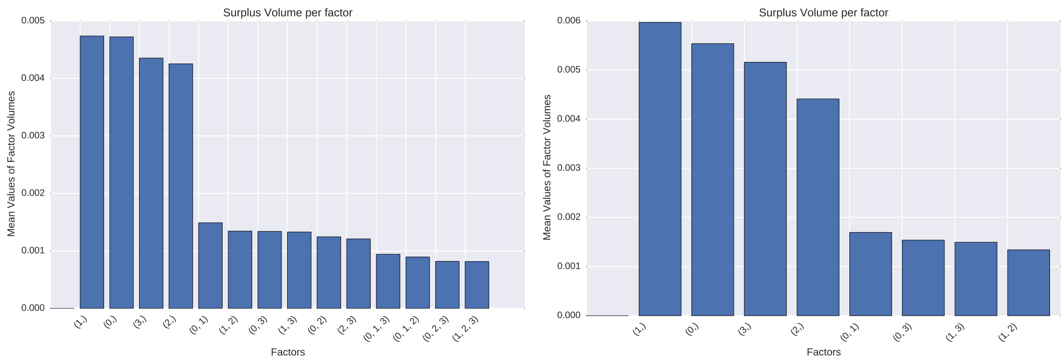

Figure 9: Surplus Volume per factor.

Figure 9(a) shows the surplus volumes corresponding to each factor at the end of second iteration of our algorithm. As expected, the surplus volumes corresponding to the factors decreases as the number of interactions increases. Hence the higher order interactions are less important and are deleted first. Figure 9(b) shows the factors remaining at the end of all the iterations. Figure 10(a) shows the actual structure of the dataset and figure 10(b) shows the predicted structure. The algorithm was able to identify all the important factors except one.

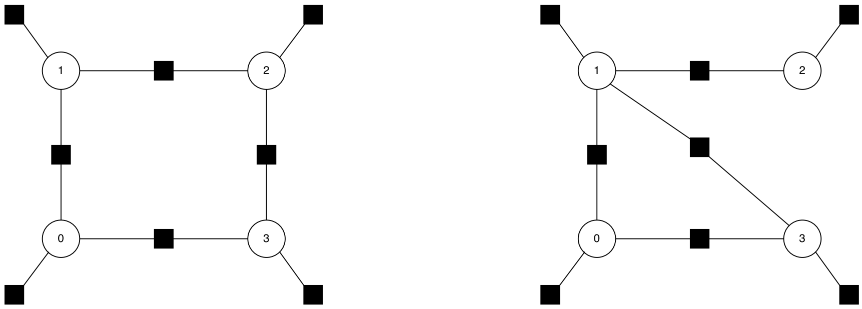

(a) Actual Structure (b) Predicted Structure

Figure 10: Underlying structure of the dataset in the form of factor graph.

We perform one more experiment with a different structure as shown in figures $12(a)$ and the predicted structure is shown in figure $12(b)$. Even in this experiment, then algorithm was able to identify the important factors to a certain extent.

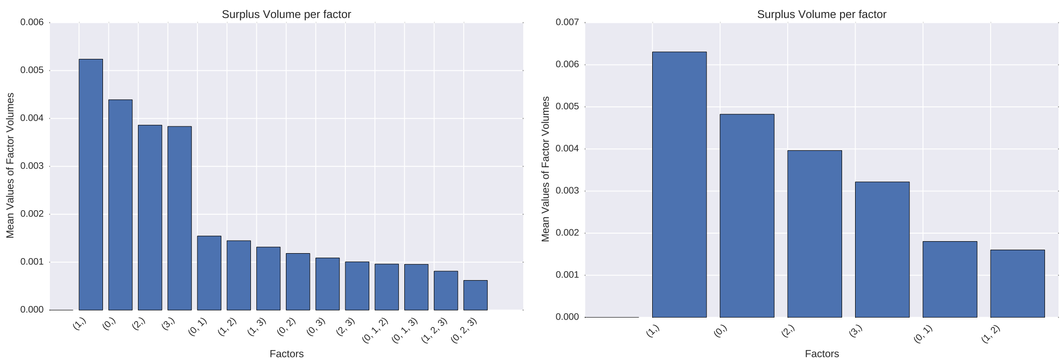

Figure 11: Surplus Volume per factor.

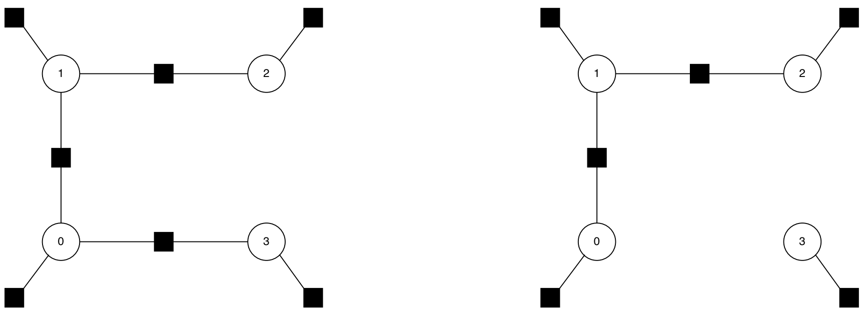

(a) Actual Structure (b) Predicted Structure

Figure 12: Underlying structure of the dataset in the form of factor graph.

As one can observe in figure 9 and 11, the surplus volumes corresponding to the factors of same interaction order does not differ much.

5 Conclusion and Future Work

Estimation of probability density using Sparse Grids and modeling the dependencies of dimensions using a factor graph which corresponds to the ANOVA decomposition, proved to be successful. There are three main outcomes of this project. First, improvement in the efficiency of the density estimation algorithm by deleting the unwanted ANOVA components from the model without much effect on the accuracy of results. Second, successful use of Markov Chain Monte Carlo sampling in estimating the expected values of sufficient statistics of the model. Third, learning the underlying structure of the dataset.

Next step would be to focus on improving the grid coarsening strategy by devicing a more accurate method to measure the importance of factors in the model. One more important improvement would be with respect to the regularization, which had a significant effect on the performance of the algorithm and hence needs to be experimented with.

References

[1] Jordan Jimmy Crabbe. Handling the curse of dimensionality in multivariate kernel density estimation. 2013.

[2] Jochen Garcke. Sparse grids in a nutshell. 2013.

[3] A G Gray and A W Moore. Nonparametric density estimation: Toward computational tractability. 2003.

[4] Michael Griebel. Sparse grids and related approximation schemes for higher dimensional problems. 2005.

[5] P Hahnen. Nichtlineare numerische verfahren zur multivariaten dichteschaetzung. 2006.

[6] Michael Griebel Hans-Joachim Bungartz. Sparse grids. 2004.

[7] M. Hegland. Adaptive sparse grids. 2003.

[8] Myles Hollander and Douglas A Wolfe. Nonparametric statistical methods. 1999.

[9] A Izenman. Recent developments in nonparametric density estimation. 1991.

[10] Eric Jones, Travis Oliphant, Pearu Peterson, et al. SciPy: Open source scientific tools for Python, 2001–. [Online; accessed 2015-07-04].

[11] Stephen J. Wright Jorge Nocedal. Numerical optimization. 1999.

[12] G Hooker M Hegland and S Roberts. Finite element thin plate splines in density estimation. 2000.

[13] Benjamin Peherstorfer. Model order reduction of parameterized systems with sparse grid learning techniques. 2013.

[14] B W Silverman. Density estimation for statistics and data analysis. 1986.

[15] Sebastian Soyer. Nonlinear density estimation with applications in astronomy. 2014.

[16] V Vapnik. Statistical learning theory. 1998.